Drosophila aPKC regulates cell polarity and cell proliferation in neuroblasts and epithelia

Melissa M. Rolls, Roger Albertson, Hsin-Pei Shih, Cheng-Yu Lee, and Chris Q. Doe

Institutes of Neuroscience and Molecular Biology, Howard Hughes Medical Institute, University of Oregon, Eugene, OR 97403

Cell polarity is essential for generating cell diversity and for the proper function of most differentiated cell types. In many organisms, cell polarity is regulated by the atypical protein kinase C (aPKC), Bazooka (Baz/Par3), and Par6 proteins. Here, we show that *Drosophila aPKC* zygotic null mutants survive to mid-larval stages, where they exhibit defects in neuroblast and epithelial cell polarity. Mutant neuroblasts lack apical localization of Par6 and Lgl, and fail to exclude Miranda from the apical cortex; yet, they show normal apical crescents of Baz/Par3, Pins, Inscuteable, and Discs large and normal spindle orientation. Mutant imaginal disc epithelia have defects in apical/basal cell polarity and tissue morphology. In addition, we show that *aPKC* mutants show reduced cell proliferation in both neuroblasts and epithelia, the opposite of the *lethal giant larvae* (*lgl*) tumor suppressor phenotype, and that reduced aPKC levels strongly suppress most *lgl* cell polarity and overproliferation phenotypes.

Introduction

Cell polarity is essential for the function of many cell types, as well as for generating cell diversity through asymmetric cell division. Over the past few years, it has become clear that cell polarity in many cell types and organisms is regulated by the evolutionarily conserved protein complex containing Baz/Par3 (Par3 in *Caenorhabditis elegans*, Bazooka in *Drosophila*, ASIP in mammals), Par6, and atypical protein kinase C (PKC-3 in *C. elegans,* aPKC in *Drosophila*, and PKCζ and λ in mammals; Doe, 2001; Ohno, 2001; Wodarz, 2002). The Baz/Par3 and Par6 proteins contain PDZ protein interaction domains, whereas aPKC is a serine/threonine kinase (Etemad-Moghadam et al., 1995; Hung and Kemphues, 1999; Suzuki et al., 2001). Each of the Baz/Par3, Par6, and aPKC proteins is reported to bind the others in vitro (Tabuse et al., 1998; Joberty et al., 2000; Lin et al., 2000; Wodarz et al., 2000; Suzuki et al., 2001; Betschinger et al., 2003), and the three proteins are reported to be interdependent for their normal localization in *C. elegans* blastomeres (Etemad-Moghadam et al., 1995; Tabuse et al., 1998; Hung and Kemphues, 1999), mammalian epithelia (Joberty et al., 2000; Suzuki et al., 2001), and *Drosophila* epithelia and neuroblasts (Wodarz et al., 2000; Petronczki and Knoblich, 2001).

The Baz/Par3–Par6–aPKC complex was initially characterized for its role in the proper partitioning of cell fate determinants during the asymmetric cell division of early blastomeres in *C. elegans*. In this system, the Par3–Par6–aPKC complex is localized to the anterior cortex of the one-cell embryo and is required to restrict the Par1 and Par2 proteins to the opposite posterior cell cortex (Kemphues, 2000). Analyses of cell polarity in other systems and cell types have shown the Baz/Par3–Par6–aPKC complex to be a widely used and flexible set of proteins that functions in conjunction with many proteins other than Par1 and Par2.

In *Drosophila*, epithelial cells have an apical/basal polarity that is reflected in the establishment of an apical membrane domain, apical adherens junctions, slightly more basal septate junctions, and a basolateral membrane domain (Tepass et al., 2001). The Baz/Par3–Par6–aPKC protein complex is targeted to the apical membrane domain, and is enriched at the adherens junctions (Tepass et al., 1990; Kuchinke et al., 1998; Wodarz et al., 2000; Bachmann et al., 2001; Hong et al., 2001; Petronczki and Knoblich, 2001).

A modified form of apical/basal polarity is present in mitotic *Drosophila* neuroblasts, where it is used to generate cellular diversity by asymmetric cell division. *Drosophila* neuroblasts divide asymmetrically along their apical/basal axis to regenerate an apically positioned neuroblast and bud off a smaller basally positioned ganglion mother cell

M. Rolls and R. Albertson contributed equally to this paper.

Address correspondence to Chris Q. Doe, Institutes of Neuroscience and Molecular Biology, Howard Hughes Medical Institute, 1254 University of Oregon, Eugene, OR 97403. Tel.: (541) 346-4877. Fax: (541) 346-4736. email: cdoe@uoneuro.uoregon.edu

Key words: Lgl; asymmetric cell division; Miranda; apical/basal polarity; Par complex

Abbreviations used in this paper: aPKC, atypical protein kinase C; Dlg, Discs large; Ecad, E-cadherin; GMC, ganglion mother cell; Insc, Inscuteable; Lgl, Lethal giant larvae; Scrib, Scribble.

(GMC). The GMC undergoes one subsequent cell division to generate neurons or glia (Goodman and Doe, 1993). The neuroblast apical domain is derived from the epithelial apical domain during the process of neuroblast delamination, and shows apical localization of the Baz/Par3–Par6–aPKC proteins during mitosis. Unlike epithelial cells, neuroblasts contain the protein Inscuteable (Insc), which is required to maintain apical localization of the Baz/Par3–Par6–aPKC proteins (Schober et al., 1999; Wodarz et al., 1999, 2000; Petronczki and Knoblich, 2001; Albertson and Doe, 2003). These proteins are required to establish a basal domain in mitosis. Among others, the Miranda protein and its cargo Prospero transcription factor and Staufen RNA-binding protein are localized to this domain (Doe and Bowerman, 2001).

A second group of proteins—Discs large (Dlg), Scribble (Scrib), and Lethal giant larvae (Lgl)—has been shown to regulate apical/basal cell polarity in *Drosophila* epithelia and neuroblasts (Bilder et al., 2000; Bilder and Perrimon, 2000; Ohshiro et al., 2000; Peng et al., 2000; Albertson and Doe, 2003). Members of this complex are rich in protein–protein interaction domains. Dlg contains one SH3 and three PDZ domains (Woods and Bryant, 1991), Lgl contains four WD40 repeats (Strand et al., 1994), and Scrib contains four PDZ domains as well as sixteen leucine-rich repeats (Bilder and Perrimon, 2000). Dlg and Scrib interact with a common binding protein called Gukholder (Mathew et al., 2002); Lgl has not been shown to physically interact with any other member of the group. In *Drosophila* epithelia, Dlg, Lgl, and Scrib are localized to the septate junction and basolateral membrane domain, where they are required for restricting the Baz/Par3–Par6–aPKC complex to the apical membrane domain (Bilder and Perrimon, 2000). In mitotic neuroblasts, Dlg, Scrib, and Lgl proteins localize to the cortex with apical enrichment, and are required for targeting basal proteins to the cortex (Ohshiro et al., 2000; Peng et al., 2000; Albertson and Doe, 2003). Their functions in addition to basal protein targeting include limiting cell proliferation (Humbert et al., 2003) and promoting spindle asymmetry in neuroblasts (Albertson and Doe, 2003). Recently, a connection has been made between the Baz/Par3–Par6–aPKC complex and the Dlg/Scrib/Lgl group of proteins. In both *Drosophila* and mammals, it has been shown that aPKC directly binds and phosphorylates Lgl (Betschinger et al., 2003; Yamanaka et al., 2003). In mammals, this phosphorylation is proposed to regulate epithelial tight junction formation (Yamanaka et al., 2003), and in *Drosophila* to regulate neuroblast basal protein targeting (Betschinger et al., 2003). Here, we investigate the role of aPKC in regulating cell polarity and cell proliferation in *Drosophila*, and the genetic interactions between *aPKC* and *lgl*. We conclude that aPKC is required for proper apical/basal polarity in neuroblasts and epithelia; that Baz/Par3 and aPKC have distinct functions in neuroblasts; and that a major function of aPKC is to suppress Lgl activity.

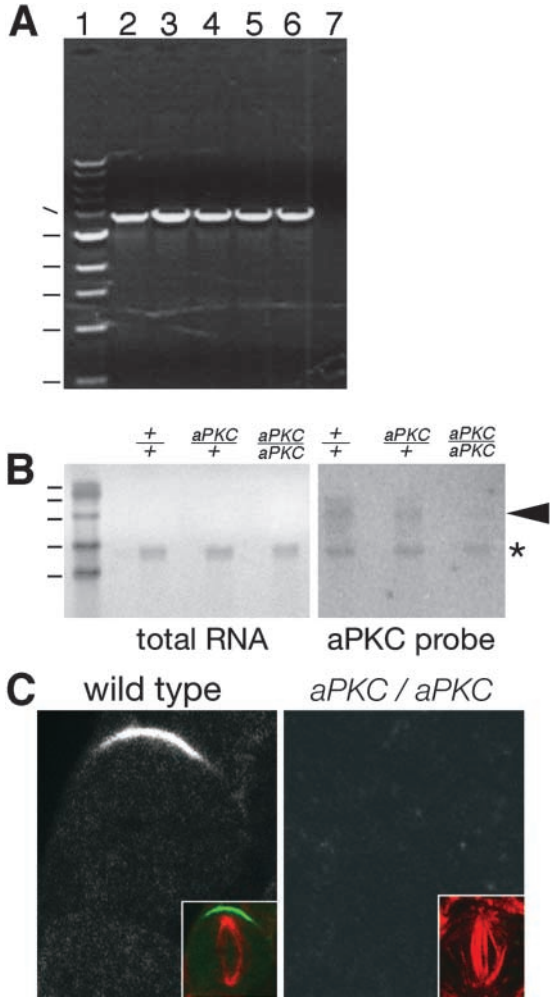

Figure 1. **Characterization of the *aPKC*^{k06403} allele.** (A) Confirmation of the *aPKC*^{k06403} allele. A pair of PCR primers, one in the P element and one in the *aPKC* gene, was used to detect the P element insertion in single-mutant *aPKC* lines (lanes 3 and 4), *lgl, aPKC* lines (lanes 2 and 5), and an *FRTG13 aPKC* line (lane 6), but not when template genomic DNA was generated from a line containing a different transposon insertion (lane 7). Mol wt markers from bottom to top: 0.5, 1, 1.5, 2, 3, and 4 kb. (B) Northern blot to detect aPKC transcript in wild-type, heterozygous *aPKC*^{k06403}, and homozygous *aPKC*^{k06403} second larval instar brains. Total RNA was visualized with ethidium bromide (left). The major band is likely rRNA. The mol wt markers from bottom to top: 1,350, 2,370, 4,400, 7,460, and 9,490 nucleotides. The major component of total RNA bound some aPKC probes, presumably nonspecifically (star). Higher mol wt products detected likely represent different aPKC transcripts (arrowhead), and are greatly reduced in the homozygous mutant brains. (C) Antibody staining reveals no full-length aPKC protein in *aPKC*^{k06403} second larval instar brain neuroblasts. Staining shows aPKC in main panels (green in inset) and tubulin (red in inset).

Results

aPKC zygotic mutant embryos have normal epithelial and neuroblast polarity

It was previously reported that embryos homozygous for the *aPKC*^{k06403} allele, which contains a P element inserted into the third intron of the *aPKC* gene, died before gastrulation (Wodarz et al., 2000). We used the same *aPKC*^{k06403} mutation, but found that homozygous mutants survived to mid-larval stages (Table I). We verified the presence of the *aPKC*^{k06403} mutant allele on all single- and double-mutant chromosomes by PCR (Fig. 1 A). To further understand the *aPKC*^{k06403} mutant allele, we assayed aPKC mRNA and protein levels in homozygous mutant larvae. Northern blots of homozygous mutant second instar larval brain tissue revealed much reduced levels of aPKC mRNA (Fig. 1 B), and

Table I. ***aPKC^{k06403}* is a genetic null mutation: *aPKC^{k06403}/aPKC^{k06403}* and *aPKC^{k06403}/Df(2R)JP1* have indistinguishable phenotypes**

Genotypes[a]	WT	*aPKC^{k06403}/aPKC^{k06403}*	*aPKC^{k06403}/Df(2R)JP1*
Metaphase NB (Miranda)[b]	*n* = 43	*n* = 53	*n* = 67
basal cortex	95%	0%	0%
basal + weak apical	5%	21%	18%
uniform cortical	0%	79%	82%
Telophase NB (Miranda)[b]	*n* = 27	*n* = 18	*n* = 40
basal cortex	100%	0%	0%
basal + weak apical	0%	44%	50%
uniform cortical	0%	56%	50%
Lethal phase	Adult	L2	L2
Larval locomotion[c]	Normal	Unc	Unc

[a]Wild type (WT) is *yellow white*; *Df(2R)JP1* removes the entire *aPKC* locus.
[b]Neuroblast phenotype was assayed in early second instar larval brains.
[c]Locomotion was evaluated 72 h after larval hatching at RT, at which time wild type were third instar larvae and both mutant genotypes were developmentally arrested second instar larvae. Unc, uncoordinated.

antibody staining showed no detectable full-length protein in late second instar brain or imaginal disc tissue (Fig. 1 C; unpublished data). Thus, the *aPKC^{k06403}* allele is close to a molecular null allele. To determine if *aPKC^{k06403}* behaves as a genetic null allele, we compared *aPKC^{k06403}/aPKC^{k06403}* to *aPKC^{k06403}/Df(2R)JP1* (a deficiency that removes the entire

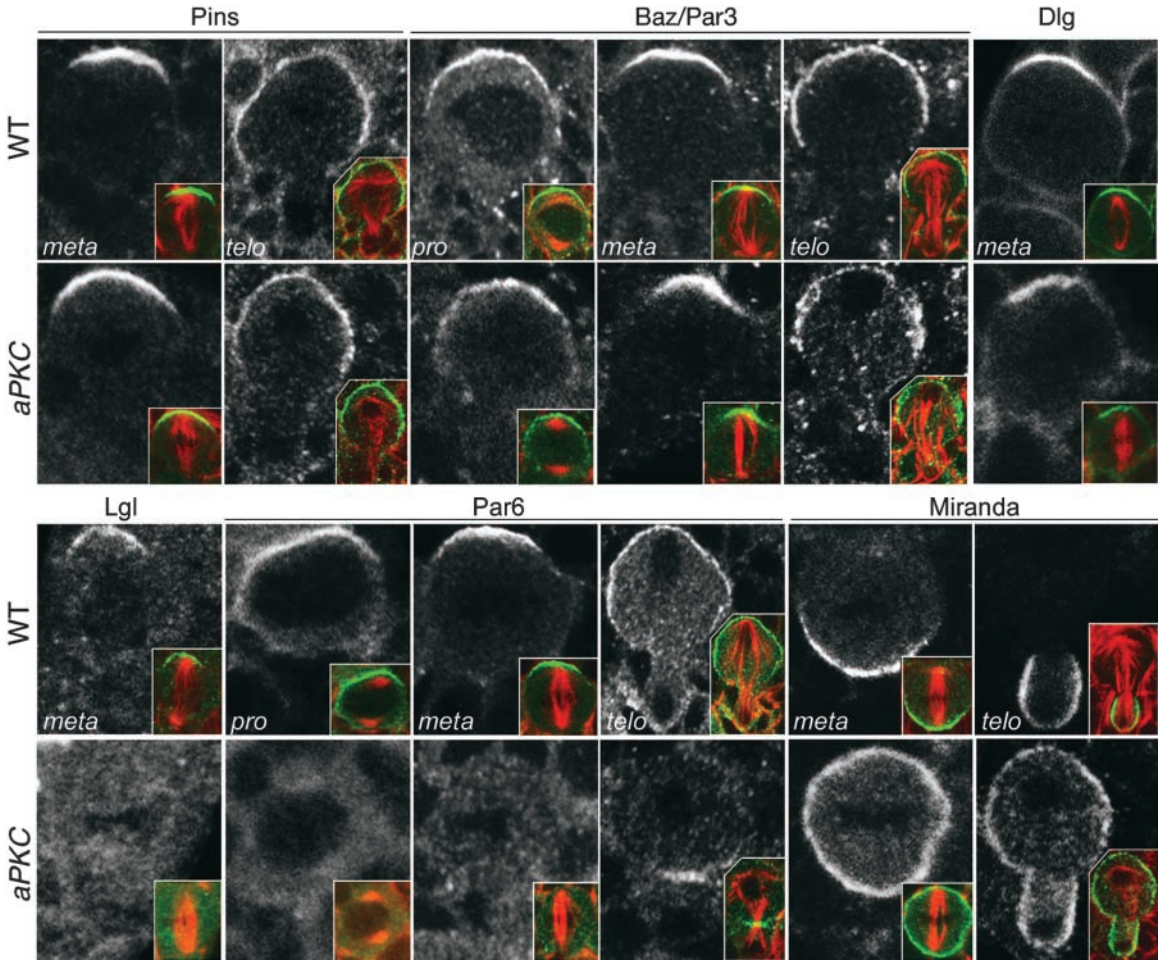

Figure 2. ***aPKC* zygotic null mutant larvae have defects in neuroblast cell polarity.** Second instar larval neuroblasts; apical cortex to the top; cell cycle stage indicated; insets show double labels for the indicated protein (green) and α-tubulin (red) to document cell cycle stage and spindle orientation. Wild-type larval neuroblasts (first and third rows): aPKC, Pins, Baz/Par3, Lgl, and Par6 are localized to the apical cortex, whereas Miranda is localized to the basal cortex. *aPKC* mutant neuroblasts (second and fourth rows): aPKC is undetectable; Baz/Par3, Pins, and Dlg are normally localized to the apical cortex; Lgl and Par6 show abnormal cytoplasmic localization (Par6 can form cortical patches at the telophase bud neck); Miranda shows abnormal uniform cortical localization.

aPKC locus) for lethal phase and neuroblast polarity phenotypes. We find indistinguishable phenotypes for both genotypes (Table I), indicating that $aPKC^{k06403}$ acts as a genetic null allele.

Stage 15 embryos homozygous for $aPKC^{k06403}$ (subsequently called *aPKC* mutants) have readily detectable maternal aPKC protein (unpublished data) and normal epithelial and neuroblast polarity, as assayed by multiple apical and basal markers (unpublished data). We conclude that zygotic aPKC is dispensable for embryonic epithelial polarity, neuroblast polarity, and embryonic viability.

aPKC zygotic mutants have defects in larval neuroblast cell polarity

aPKC zygotic mutants died as late second instar larvae, which allowed us to analyze neuroblast cell polarity in mid-second instar larval brains. In wild-type mitotic neuroblasts, we detected apical cortical localization of Baz/Par3, Pins, Lgl, and Par6 throughout mitosis (Fig. 2). *aPKC* mutant larvae were identified by the lack of GFP expression from the balancer chromosome. In these mutants, Par6 and Lgl proteins were delocalized into the cytoplasm in all metaphase neuroblasts; the only enrichment of either protein was faint ectopic Par6 at the cleavage furrow in telophase (Fig. 2). In contrast, all mutant neuroblasts showed normal apical localization of Baz/Par3, Pins, and Dlg proteins (Fig. 2). We conclude that aPKC is essential for Lgl and Par6 apical localization, but is not required for Baz/Par3, Insc, Pins, or Dlg apical localization.

Next, we investigated the role of aPKC in basal protein localization in second instar larval neuroblasts. In the wild type, Miranda protein is localized to the basal cortex from prometaphase through telophase, ultimately being partitioned specifically into the basal GMC (Fig. 2). In *aPKC* mutants at late second instar (when the larvae become uncoordinated), Miranda is localized around the entire cortex from metaphase through telophase in all neuroblasts examined (Fig. 2); earlier in second instar (when larvae are moving normally), about half the neuroblasts still showed weak basal enrichment at telophase (Table I). We conclude that aPKC function is required to exclude Miranda from the apical cortex of the neuroblast, even during telophase when basal localization becomes Baz/Par3-independent (Schober et al., 1999; Peng et al., 2000; Albertson and Doe, 2003; Cai et al., 2003).

It is commonly accepted that the Baz/Par3–Par6–aPKC complex is required for orienting the neuroblast mitotic spindle orthogonal to the overlying ectodermal cell layer, thus reliably placing the GMCs toward the inside of the embryo (Doe and Bowerman, 2001; Jan and Jan, 2001; Ahringer, 2003). We could not assay the role of aPKC in embryonic neuroblast spindle orientation due to the large pool of maternal aPKC protein, but we did assay spindle orientation in *aPKC* mutant larval neuroblasts. We observed that

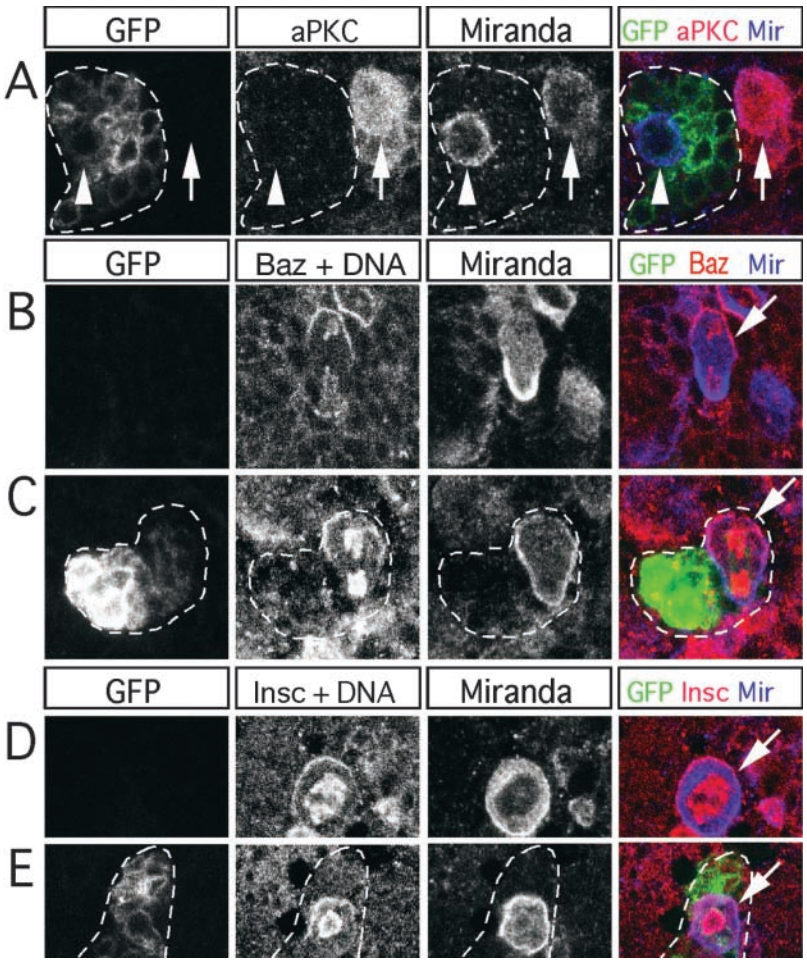

Figure 3. **Positively marked *aPKC* null mutant clones reveal defects in neuroblast cell polarity.** A MARCM strategy was used to generate *aPKC* mutant clones positively marked by mCD8::GFP (indicated by dashed surrounding lines) in brains of *aPKC*/+ heterozygous animals. First column shows GFP marking the mutant clones (levels are low in neuroblasts, but can be readily detected when viewed at higher gain; not depicted); second column shows a DNA marker (phosphohistone H3) and/or apical polarity proteins; third column shows Miranda staining to identify neuroblasts and to assay basal protein targeting. (A) Neuroblast within an *aPKC* mutant clone lacks detectable aPKC protein (arrowhead); wild-type neuroblast outside the clone has high levels of aPKC protein (arrow). Neuroblasts are at interphase and aPKC is cytoplasmic. (B) Wild-type anaphase neuroblast shows normal apical Baz/Par3 (arrow) and basal Miranda. (C) *aPKC* mutant anaphase neuroblast shows normal apical Baz/Par3 (arrow), but Miranda is abnormally localized uniformly around the cortex. (D and E) Both wild-type and mutant prophase neuroblasts show normal apical Insc (arrows); Miranda is not strongly localized at this stage of the cell cycle.

the metaphase spindle was always centered on the apical Baz/Par3 crescent in these mutant neuroblasts (Fig. 2, insets). Thus, aPKC is not required for aligning the mitotic spindle along the intrinsic axis of apical/basal polarity within larval neuroblasts, and it is likely that Par6 is also dispensable, as it is completely delocalized in *aPKC* mutants.

To determine the cell-autonomous aPKC phenotype, and to determine whether a more severe neuroblast phenotype could be observed when neuroblast life was not curtailed by larval death, we generated *aPKC* mutant clones. The MARCM system (Lee and Luo, 2001) was used to generate positively marked mutant clones in 0–12-h *aPKC*/+ first instar larvae, and the phenotype was assayed in third larval instar brains. By this time, aPKC was completely undetectable in neuroblasts within the clone (Fig. 3 A, arrowhead). Wild-type neuroblasts outside the clone (*aPKC*/+ or +/+) showed normal apical Insc, apical Baz/Par3, and basal Miranda localization (Fig. 3, B and D). As in mutant brains, Baz/Par3 and Insc proteins were localized normally to the apical neuroblast cortex (Fig. 3, C and E), and Miranda lost its normal restriction to the basal cortex (Fig. 3 C). We conclude that aPKC is essential for Par6 and Lgl apical localization and for excluding Miranda from the apical cortex, but it has no role in apical localization of Baz/Par3, Insc, Pins, Dlg, or in spindle orientation.

aPKC zygotic mutant larvae have defects in epithelial cell polarity

We assayed epithelial cell polarity in wild-type and *aPKC* zygotic mutant eye imaginal discs, which were identified based on their characteristic connection to the larval brain via the optic nerve (Fig. 4 C, brackets). Wild-type (*aPKC*/+) second larval instar eye disc epithelia formed a smoothly folded cellular monolayer, and showed the expected distribution of apical/basal cell polarity markers; aPKC and Discs lost were localized to the apical plasma membrane, E-cadherin (Ecad) was localized to the subapical adherens junctions, and Dlg was localized to the even more basal septate junction and basolateral membrane domain (Fig. 4 A; unpublished data). In contrast, *aPKC* mutant second larval instar eye imaginal discs were not organized into an epithelial monolayer (Fig. 4, B–D). There was no detectable aPKC protein, and Ecad/Dlg staining was less intense than in the wild type (Fig. 4 B), either because the proteins were more widely distributed or because there was less protein present. When the gain was increased to visualize the low levels of Ecad and Dlg proteins, we observed Ecad and Dlg proteins distributed around the cell cortex rather than confined to their normal apical/basal domain (Fig. 4, C and D; unpublished data). Thus, the *aPKC* mutant eye imaginal disc epithelia appear to have a loss of epithelial polarity characterized by unpolarized cortical distribution of an apical adherens junction marker (Ecad) and a basolateral marker (Dlg).

aPKC is required for cell proliferation in neuroblasts and epithelia

During the course of analyzing the *aPKC* mutant clones, we observed a dramatic decrease in the number of neuronal progeny in the positively marked *aPKC* mutant clones compared with positively marked wild-type control clones. We focused our analysis on the well-characterized mushroom body neuroblasts: each neuroblast first generates neurons

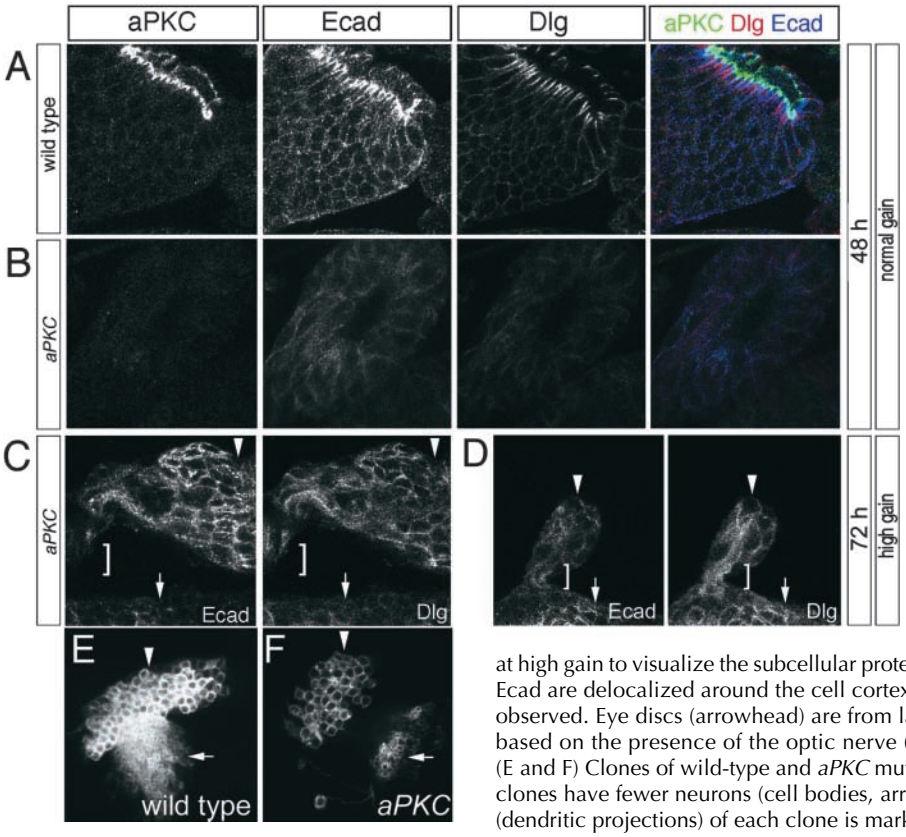

Figure 4. ***aPKC* zygotic null mutants have defects in larval epithelial cell polarity.** (A and B) *aPKC* mutant epithelia show decreased levels of apical/basal cell polarity markers. Wild-type (A) and *aPKC/aPKC* mutant (B) eye imaginal discs 48 h after larval hatching (second instar larvae). Apical/basal polarity is assayed using the apical marker aPKC (green), the apical adherens junctions marker E-cadherin (Ecad; blue), and the septate junction and basolateral membrane marker Dlg (red). Wild-type imaginal disc epithelia show well defined apical/basal polarity, normal disc morphology, and form a smooth monolayer; aPKC mutant imaginal discs show no detectable aPKC and reduced Dlg and Ecad levels. Discs in A and B were stained in parallel and imaged at the same confocal settings to allow protein levels to be compared. (C and D) *aPKC* mutant epithelia with extremely small disc size, defects in apical/basal polarity, and loss of epithelial monolayer morphology. Discs are imaged at high gain to visualize the subcellular protein distribution and disc morphology. Dlg and Ecad are delocalized around the cell cortex, although occasional clusters of Ecad were observed. Eye discs (arrowhead) are from late second instar larvae and were identified based on the presence of the optic nerve (brackets) connecting to the brain (arrow). (E and F) Clones of wild-type and *aPKC* mutant mushroom body neurons. aPKC mutant clones have fewer neurons (cell bodies, arrowheads) than wild-type clones. The calyx (dendritic projections) of each clone is marked by arrows.

that send axons into the γ lobe of the adult mushroom body, and subsequently switches to producing neurons that have axon projections into the α and β lobes (Lee et al., 2000). We found that wild-type clones contained 300–400 neurons ($n = 2$), consisting of early-born γ neurons as well as later-born α and β neurons (Fig. 4 E). In contrast, *aPKC* clones contained 75–125 neurons ($n = 3$), and consisted primarily of early-born γ neurons (Fig. 4 F). Because few α and β neurons were present in the mutant clones, the most likely explanation for reduced clone size is the cessation of neuroblast division just after the early-born γ neurons were produced. A similar defect in cell proliferation was observed in *aPKC* mutant eye imaginal discs: *aPKC* mutant discs were always much smaller than normal second instar eye discs (Fig. 4, C and D), although the animals remained as second instar larvae for at least twice as long as normal. Thus, aPKC is required to maintain cell proliferation of larval neuroblasts and imaginal disc epithelial cells.

aPKC and *lgl* show dosage-sensitive negative genetic interactions

aPKC binds and phosphorylates Lgl in both mammals and *Drosophila* (Betschinger et al., 2003; Yamanaka et al., 2003), so we investigated possible genetic interaction between *aPKC* and *lgl* in regulating cell polarity and cell proliferation. First, we examined whether reduced *aPKC* could suppress an *lgl* neuroblast cell polarity phenotype in stage 15 embryos. In wild-type neuroblasts, Miranda was localized to the basal cortex, but in lgl^4 mutants (which retain low levels of maternal Lgl protein; unpublished data), neuroblasts were observed with Miranda delocalized from the cortex into the cytoplasm and onto the mitotic spindle (Fig. 5, A and B; Table II). In contrast, lgl^4 aPKC double mutant embryos showed a clear suppression of the lgl^4 polarity phenotype, with more Miranda basal crescents than lgl^4 single mutants (Fig. 5 C; Table II).

To test whether reduced aPKC levels could suppress the *lgl* brain tumor phenotype, we examined brain size and neuroblast numbers in early third instar larvae 74 h after larval hatching. Wild-type brains contained an average of 90 neuroblasts, but similarly staged *lgl* mutant brains were larger

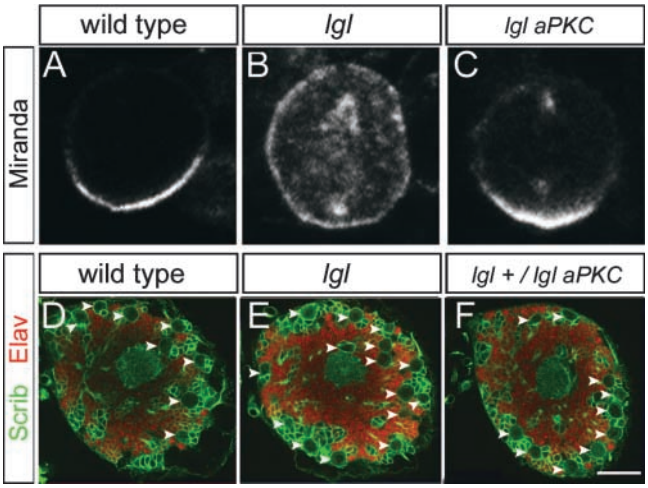

Figure 5. **Reduced aPKC levels suppress the *lgl* neuroblast polarity and brain tumor phenotypes.** (A–C) Reduced aPKC levels suppress the *lgl* neuroblast polarity phenotype in embryonic stage 15 neuroblasts. (A) In the wild type, Miranda is localized to the basal cortex. (B) In lgl^4/lgl^4 mutants, Miranda is predominantly delocalized into the cytoplasm and onto the mitotic spindle and centrosomes. (C) In lgl^4 *aPKC*/lgl^4 aPKC double mutants, there is noticeably more basal Miranda localization than in lgl^4/lgl^4 single mutants, although some cytoplasmic/spindle association remains. See Table II for quantification. (D–F) Reduced aPKC levels suppress the *lgl* brain tumor phenotype. (D) Wild type, (E) lgl^{334}/lgl^{334}, and (F) lgl^{334}+/lgl^{334} *aPKC*. Third instar larval brains 74 h after hatching were stained for the Scrib membrane marker (green) to identify neuroblasts (large cells, arrowheads) and GMCs (smaller cells), and with Elav (red) to mark neurons. In each panel, the optical cross section was taken at the same level, just apical to the mushroom body. See Table II for quantitation. Bar, 25 μm.

and possessed ∼135 neuroblasts (Fig. 5, D and E; Table II). When aPKC levels were reduced by 50% (*lgl aPKC*/*lgl*+), we observed a clear reduction in brain size and neuroblast number (Fig. 5 F; Table II). Thus, reduced aPKC levels suppressed the *lgl* brain tumor phenotype as well as the *lgl* neuroblast cell polarity phenotype.

Next, we tested whether reduced aPKC activity could suppress the previously described *lgl* epithelial cell polarity phenotype (Bilder et al., 2000). In wild-type larvae, late third

Table II. **Reduced aPKC suppresses Lgl cell polarity and cell overgrowth phenotypes**

Genotypes[a]	WT	*lgl*/*lgl*	*lgl aPKC*/*lgl aPKC* or *lgl aPKC*/*lgl*+
NB basal Miranda (E10)[b]	94%	33%	72%
NB basal Miranda (E15)[b]	94%	7%	24%
Large NB size (E15)[b,c]	100%	88%	83%
NB number (L3)[d]	92 ± 6	137 ± 10	107 ± 4
Brain size (L3)[e]	82 ± 8	136 ± 12	114 ± 11
Imaginal disc size (L3)	Normal	Enlarged	Normal
Imaginal disc monolayer (L2/3)	Yes	Never	Yes

[a]The wild-type (WT) stock were *y w* (rows 1–3), lgl^{334} $aPKC^{k06403}$/++ (rows 4 and 7), and lgl^{334}/+ (rows 5 and 6). The *lgl*/*lgl* mutants were lgl^4/lgl^4 (rows 1–3), lgl^4/lgl^{334} (row 5), and lgl^{334}/lgl^{334} (rows 4, 6, and 7). The *lgl aPKC* double mutants were lgl^4 $aPKC^{k06403}/lgl^4$ $aPKC^{k06403}$ (rows 1–3), lgl^{334} $aPKC^{k06403}/lgl^4$+ (row 5), and lgl^{334} $aPKC^{k06403}/lgl^{334}$+ (rows 4, 6, and 7).
[b]Number of neuroblasts (NB) scored is >41 for all genotypes.
[c]NB/GMC cell size ratio of >0.8 at telophase (Albertson and Doe, 2003).
[d]Neuroblast number per hemisphere; $n = 10$ for each genotype.
[e]Brain size in volume ($mm^3 \times 10^{-4}$) per hemisphere; $n = 10$ for each genotype.

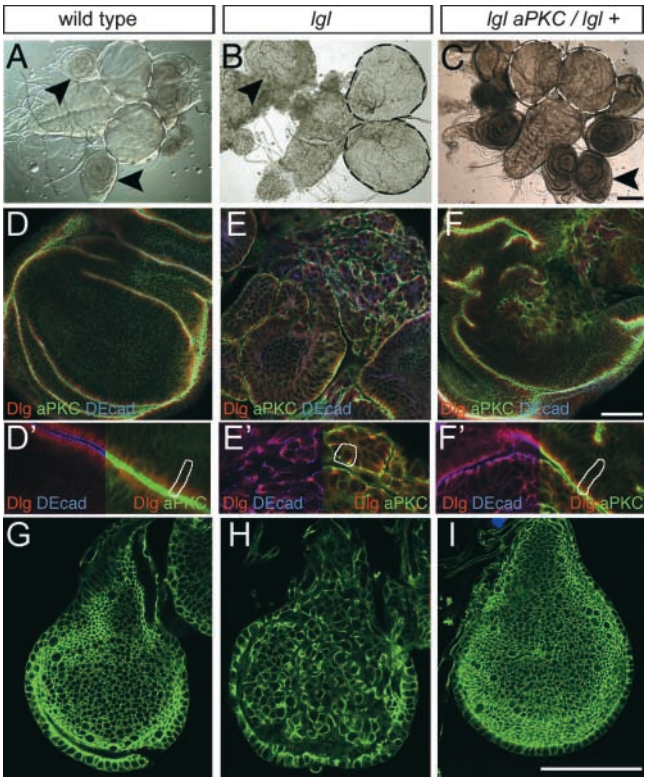

Figure 6. ***aPKC* suppresses the *lgl* epithelial polarity phenotype.** (A–C) Low magnification view of a third instar larval nervous system (brain lobes outlined) and leg discs (arrowheads), fixed 74 h after hatching at 25°C. (A) In the wild type, imaginal discs are highly ordered. (B) In lgl^{334}/lgl^{334} larvae, the discs are large, disorganized, and fused with surrounding tissue. (C) In lgl^{334} *aPKC*/lgl^{334}+ larvae, the discs recover nearly normal morphology. (D–F) Confocal optical section of similarly staged third instar wing discs stained for the apical marker aPKC (green), the apical adherens junction marker Ecad (blue), and the septate junction and basolateral marker Dlg (red). Higher magnification views are shown below. Individual cells are outlined in D′–F′. (D and D′) Wild-type epithelia. (E and E′) lgl^{334} discs lose their gently folded monolayer morphology, but individual cells still show normal topology of the apical/basal markers. However, the size of the apical domain appears enlarged at the expense of the basolateral domain. (F and F′) In lgl^{334} *aPKC*/lgl^{334}+, the imaginal discs have nearly normal morphology and relative size of the apical and basolateral membrane domains. (G–I) Confocal optical section of second instar wing discs stained for Scrib (green) to visualize cell outlines and tissue morphology. (G) Wild-type discs are unfolded epithelial monolayer. (H) In lgl^{334} discs, the cells are rounder and form a multilayer aggregate in the center of the disc. (I) In lgl^{334} *aPKC*/lgl^{334}+, the imaginal discs recover nearly normal morphology. Bars: 100 μm (A–C); 50 μm (D–I).

instar leg and wing imaginal discs have a well-defined morphology (Fig. 6 A) with a smooth monolayer of columnar cells that have a clear apical/basal polarity (Fig. 6, D and D′). In contrast, lgl^{334} mutant third instar imaginal discs are highly disorganized and often fused with each other or nearby tissues (Fig. 6 B); at the cellular level, mutant epithelial cells are round instead of columnar, with an expanded apical membrane domain (Fig. 6, E and E′). Strikingly, lgl^{334} mutants that are heterozygous for an *aPKC* mutation have a nearly normal late third instar leg and wing imaginal disc morphology (Fig. 6 C), including columnar cell shape and an approximately normal apical membrane domain (Fig. 6, F and F′; Table II). In addition, we characterized an earlier stage of imaginal disc development (early third instar; 74 h after larval hatching at 25°C). We find that *lgl* mutants already show morphological disorganization of imaginal discs (Fig. 6 H), but both wild-type and *lgl aPKC/lgl*+ mutants show essentially normal leg and wing imaginal disc morphology (Fig. 6, G and I; unpublished data). We conclude that reduced aPKC levels can suppress the *lgl* epithelial cell polarity phenotype.

Are all *lgl* phenotypes suppressed by reduced aPKC levels? Recently, we have shown that ~12% of the neuroblasts in lgl^{4} homozygotes have a reduced apical cortical domain and apical spindle poles, leading to an inverted asymmetric division and a smaller neuroblast size (Albertson and Doe, 2003). This *lgl* phenotype was not suppressed by reducing aPKC levels, and in fact may have been slightly enhanced (Table II, row 3). The inability of *aPKC* mutation to suppress the *lgl* "small neuroblast" or "inverted division" phenotype is consistent with a recent observation that aPKC positively regulates neuroblast cell size (Cai et al., 2003). Thus, aPKC and Lgl appear to cooperate to positively regulate neuroblast cell size, despite their negative interaction in regulating other aspects of cell polarity.

Discussion

It was previously reported that $aPKC^{k06403}$ zygotic mutant embryos died before gastrulation and that all epithelial and neuroblast polarity was lost (Wodarz et al., 2000). We find a much later onset phenotype: survival of $aPKC^{k06403}$ homozygotes to second larval instar with no significant embryonic phenotype. Although surprising, we feel our results reflect the authentic zygotic $aPKC^{k06403}$ mutant phenotype for several reasons. First, recent work from the Wodarz lab confirms that $aPKC^{k06403}$ homozygotes survive to at least late embryonic stages without significant epithelial or neuroblast defects (Wodarz, A., personal communication), presumably due to the absence of deleterious second site mutations that were on the original $aPKC^{k06403}$ chromosome. Second, we used PCR to verify the presence of the $aPKC^{k06403}$ allele in all of our stocks, and used dominantly marked balancer chromosomes to independently confirm the identity of every $aPKC^{k06403}$ homozygote that we analyzed. Third, we showed that $aPKC^{k06403}$ homozygous second instar larvae had very low levels of aPKC mRNA and no detectable full-length protein; thus, we analyzed a very strong or null *aPKC* mutant phenotype. Fourth, we showed that $aPKC^{k06403}/aPKC^{k06403}$ and $aPKC^{k06403}/Df(2R)JP1$ larvae have indistinguishable lethal phases and quantitative neuroblast phenotypes; thus, $aPKC^{k06403}$ behaves as a genetic null allele. Finally, we showed that $aPKC^{k06403}$ homozygous embryos had persistent maternal aPKC protein, explaining the lack of an embryonic phenotype in these mutants.

One of our more unexpected findings is that *aPKC* mutant neuroblasts show normal Baz/Par3 apical localization. The Baz/Par3–Par6–aPKC complex has been suggested to form a functional unit that is interdependent for localization in *C. elegans*, mammals, and *Drosophila* (Doe and Bowerman, 2001; Ohno, 2001). We find that Baz/Par3 shows normal apical localization in *aPKC* mutant neuroblasts,

showing that normal Baz/Par3 localization can occur without being part of the Par3–Par6–aPKC complex. In addition, we show that neuroblasts lacking apical aPKC and Par6 still form a molecularly defined apical cortical domain containing Baz/Par3, Insc, Pins, and Dlg. Our results allow us to propose a hierarchy for apical protein localization in neuroblasts: Baz/Par3–Insc–Pins–Dlg→aPKC→Par6–Lgl (Schober et al., 1999; Wodarz et al., 1999; Albertson and Doe, 2003). Our hierarchy is consistent with recent biochemical analyses in which a protein complex was isolated containing Par6–aPKC–Lgl, but not Baz/Par3 (Betschinger et al., 2003; Yamanaka et al., 2003). We suggest that aPKC may be required to anchor the Par6–aPKC–Lgl complex at the apical cortex of the neuroblast.

Both aPKC and Lgl are required for Miranda basal localization in neuroblasts, and all available data support a model in which Lgl is required for targeting Miranda to the neuroblast cortex, whereas aPKC blocks Lgl function on the apical side of the neuroblast. First, *lgl* mutants have little or no Miranda at the cortex (Ohshiro et al., 2000; Peng et al., 2000; Albertson and Doe, 2003). Second, *aPKC* mutants show uniform cortical Miranda localization (this paper). Third, a weak *lgl* phenotype can be suppressed by reducing aPKC levels, showing that aPKC activity antagonizes Lgl activity (this paper). Fourth, aPKC and Lgl physically interact (Betschinger et al., 2003). Finally, an overexpressed nonphosphorylatable Lgl protein is uniformly cortical and able to induce uniform cortical Miranda localization, whereas phospho-Lgl is preferentially released from the cell cortex (Kalmes et al., 1996; Betschinger et al., 2003). This has led to a model in which Lgl acts as an anchor for Miranda at the basal cortex, but is absent from the apical cortex due to aPKC-mediated phosphorylation (Betschinger et al., 2003). Although this simple model is attractive, we note that Lgl has never been observed colocalized with Miranda in a basal cortical crescent (Ohshiro et al., 2000; Peng et al., 2000; Albertson and Doe, 2003; Betschinger et al., 2003), and a role for cytoplasmic Lgl in Miranda localization has not been definitively ruled out.

The Baz/Par3–Par6–aPKC complex has a well-characterized role in regulating neuroblast spindle orientation (Doe and Bowerman, 2001; Jan and Jan, 2001; Knoblich, 2001; Ahringer, 2003). Spindle orientation can be measured relative to extrinsic landmarks around the neuroblast (e.g., perpendicular to the overlying ectoderm) or relative to intrinsic cues within each neuroblast (e.g., perpendicular to the Baz/Par3–Par6–aPKC apical crescent). Mutations in *baz* or *par6* genes randomize embryonic neuroblast spindle orientation relative to the overlying ectoderm (Kuchinke et al., 1998; Wodarz et al., 1999; Petronczki and Knoblich, 2001), but it is not clear whether these phenotypes are due to disruption of the ectodermal layer or to a cell-autonomous defect in the neuroblast. We cannot assay the function of aPKC in embryonic neuroblast spindle orientation due to high levels of maternal aPKC protein present in *aPKC* zygotic mutant embryos. However, we do show that aPKC is not required for intrinsic spindle orientation in larval neuroblasts; the mitotic spindle is always perpendicular to the Baz/Par3–Insc–Pins apical crescent.

The Baz/Par3 and Par6 proteins are required to establish epithelial polarity in *Drosophila* (Muller and Wieschaus, 1996; Schober et al., 1999; Wodarz et al., 1999; Petronczki and Knoblich, 2001), and we show here that aPKC is also required for normal apical/basal epithelial cell polarity. The similar phenotype in *baz*, *par6*, and *aPKC* mutants may indicate that these proteins function together as a complex to provide a single function in epithelia, despite the evidence that they have independent functions in neuroblasts. One primary function may be the inhibition of Lgl activity because we find that the *lgl* epithelial polarity defects can be strongly suppressed by reducing aPKC levels. Lgl–Dlg–Scrib activity can also antagonize Baz/Par3–Par6–aPKC activity (Bilder et al., 2003), and it is tempting to speculate that aPKC inactivates Lgl by phosphorylation, whereas Lgl can inactivate aPKC by sequestering it into an Lgl–Par6–aPKC complex and out of the Baz/Par3–Par6–aPKC complex (Betschinger et al., 2003; Yamanaka et al., 2003).

The role of aPKC in cell proliferation has not been previously investigated in *Drosophila*. There are three lines of evidence showing that aPKC promotes cell proliferation in neuroblasts and epithelia. We find that the number of cells in *aPKC* mutant mushroom body neuroblast clones is significantly lower than the number in wild-type clones. There appears to be a normal number of early-born γ neurons in these clones, followed by only a few later-born α and β neurons. The normal number of early-born γ neurons suggests that loss of aPKC does not lead to cell death in this population; moreover, we see no decrease in the number of neuroblasts per brain lobe in *aPKC* mutant larvae (unpublished data). We conclude that cell death is not contributing to the reduction in neurons observed in the clones, but rather, that the neuroblast stops dividing near the time the neuroblast switches over to generating α and β neurons. The neuroblast may become arrested at some point in the cell cycle, or it may undergo a terminal division to generate a pair of GMCs (perhaps due to both daughter cells inheriting Miranda and Prospero GMC determinants). A second indication that aPKC promotes cell proliferation is that we observe far fewer epithelial cells in *aPKC* mutant eye imaginal discs compared with the wild type, even with an additional day of growth as second instar larvae. Finally, we observe that a 50% reduction in aPKC levels (*aPKC*/+) can strongly suppress the epithelial and brain overproliferation phenotypes of *lgl* mutants. Together, our data show that aPKC positively regulates cell proliferation in epithelia and neuroblasts. Interestingly, reduction in the function of the mammalian atypical PKCζ (using overexpression of a dominant-negative kinase) can suppress Rac1/cdc42-induced overproliferation (Qiu et al., 2000). Thus, aPKC may have an evolutionarily conserved role in promoting cell proliferation, as well as in the establishment of cell polarity.

Although aPKC and Lgl act antagonistically to regulate many aspects of epithelial and neuroblast cell polarity and cell proliferation, they may share a common positive function in regulating neuroblast apical cell size. Previously, we showed that *lgl* zygotic mutants have some embryonic telophase neuroblasts with an abnormally small apical cortical domain, apical spindle pole, and neuroblast size (Albertson and Doe, 2003). These defects are not suppressed by reduc-

ing aPKC levels, and in fact may be enhanced (Table II). Thus, we propose that Lgl and aPKC both act positively to promote large apical cell and spindle pole size. It has been reported that Baz/Par3–Par6–aPKC and Pins–Gαi act in parallel pathways to promote large apical cell size and apical spindle size (Cai et al., 2003); Lgl could be acting as part of the Pins–Gαi pathway, or as a third input promoting apical cell and spindle size.

Materials and methods

Fly genetics and morphological analysis

The *aPKC*^{k06403}, *lgl*^{4}, *lgl*^{334}, and *Df(2R)JP1* stocks were obtained from the Bloomington Stock Center (Bloomington, IN), and rebalanced over *CyO actin::GFP*. All alleles are described in Flybase (http://flybase.bio.indiana.edu:82/).

Analytic PCR

Genomic DNA was isolated as described by the Berkeley *Drosophila* Genome Project (http://www.fruitfly.org/about/methods/inverse.pcr.html). PCR primers were designed to detect the presence of the PlacW transposon in the third intron of *aPKC* as it had been described previously (Wodarz et al., 2000). One primer was complementary to the 3′ end of the transposon (5′-CACTCGCAGTTATTGCAAGC-3′), and the other was complementary to the third exon of *aPKC* (5′-TCGCCATCGCAAGACAATCCCG-3′). PCR was performed using the Expand system (Roche).

Northern blot

RNA was isolated from second larval instar brains 48 h after hatching. Brains were dissected in Schneider's medium and immediately transferred to TRIzol® reagent (Invitrogen); RNA was isolated according to the manufacturer's directions. RNA was separated on a formaldehyde gel and transferred to zetabind membrane (Cuno, Inc.). Random-primed probe was prepared using the entire *aPKC* coding region, and the SV40 poly(A)$^{+}$ region from pUAST, as a template.

Antibody production, staining, and imaging

The Par6 antibody was generated in rats against aa 130–255. The protein fragment was isolated with a His tag that was subsequently removed. The Lgl antibody was generated against an Lgl COOH-terminal 21-aa peptide (Albertson and Doe, 2003); using our fixation protocol, this antisera detects only apical cortical Lgl protein, and not the uniform cortical or cytoplasmic protein reported for other Lgl antisera (Ohshiro et al., 2000; Peng et al., 2000).

Larvae were raised on standard food. Brains and imaginal discs were dissected in Schneider's Medium (Sigma-Aldrich), fixed for 20 min in 4% formaldehyde, and stained as described previously (Cox et al., 1996). Embryos were fixed and stained as described previously (Albertson and Doe, 2003). The primary antibodies used were mouse anti-Dlg 4F3E3 (1:100; Parnas et al., 2001), rat anti-Scribble (1:2,500; Albertson and Doe, 2003), rat anti-DE-cadherin (1:100; Oda et al., 1994), rabbit anti-aPKC (1:1,000; Santa Cruz Biotechnology, Inc.), mouse anti-α-tubulin (1:5,000; Sigma-Aldrich), rat anti-Lgl (1:150; Albertson and Doe, 2003), rabbit anti-Miranda (1:1,000; Albertson and Doe, 2003), rat anti-Par6 (1:200), rabbit anti-Baz/Par3 (1:500; Wodarz et al., 2000), rabbit anti-phosphohistone H3 (1:1,000; Upstate Biotechnology), rabbit anti-Insc (1:1,000; Kraut et al., 1996), and rabbit anti-Pins (1:1,000; Yu et al., 2000). The secondary antibodies Cy5- and Alexa® Fluor 488–conjugated goat anti–rabbit IgG, Cy5- and Alexa® Fluor 488–conjugated goat anti–rat IgG, and Cy3-conjugated goat anti–mouse IgG (Jackson ImmunoResearch Laboratories or Molecular Probes, Inc.) were used at 1:400. Samples were mounted in AquaPolymount (Polysciences, Inc.) and imaged on a confocal microscope (Radiance; Bio-Rad Laboratories). Low magnification transmitted light images of larval brains and imaginal discs were collected on a microscope (Axioplan; Carl Zeiss MicroImaging, Inc.). Confocal images were processed with ImageJ (National Institutes of Health, Bethesda, MD), and figures were assembled in Adobe Photoshop® v6.0.

Generating positively marked *aPKC* mutant clones

We used the MARCM system to generate clones (Lee et al., 2000), using stocks available from the Bloomington Stock Center. To generate mushroom body *aPKC* clones, *elavGAL4 UASmCD8 hsFlp;FRTG13 tubPGAL80* flies were crossed to *FRTG13 aPKC*^{k06403}*/CyO* flies. Heat shock of first instar larvae from this cross at 37°C for 1 h induced Flp-mediated recombination at FRT sites that generated homozygous *aPKC* clones that lacked GAL80. In these clones, GAL4-mediated transcription of *mCD8-GFP* was derepressed, thereby positively marking the mutant clones. Clones were examined in third larval instar brains and 2–5-d-old adults.

We thank the Bloomington stock center for fly stocks; Rhiannon Penkert for generating the Par6 fragment; Mike Marusich at the University of Oregon Hybridoma Lab for assistance in antibody generation; Andreas Wodarz for communicating unpublished results; and Greg Kothe for help with Northern blots. We thank Karsten Siller and Sarah Siegrist for comments on the manuscript.

This work was supported by Damon Runyon postdoctoral fellowships (to M. Rolls and C.-Y. Lee), a National Institutes of Health graduate student training grant (to R. Albertson), and by the Howard Hughes Medical Institute, where C.Q. Doe is an Investigator.

Submitted: 16 June 2003
Accepted: 15 October 2003

References

Ahringer, J. 2003. Control of cell polarity and mitotic spindle positioning in animal cells. *Curr. Opin. Cell Biol.* 15:73–81.

Albertson, R., and C.Q. Doe. 2003. Dlg, Scrib, and Lgl regulate neuroblast cell size and mitotic spindle asymmetry. *Nat. Cell Biol.* 5:166–170.

Bachmann, A., M. Schneider, E. Theilenberg, F. Grawe, and E. Knust. 2001. *Drosophila* Stardust is a partner of Crumbs in the control of epithelial cell polarity. *Nature.* 414:638–643.

Betschinger, J., K. Mechtler, and J.A. Knoblich. 2003. The Par complex directs asymmetric cell division by phosphorylating the cytoskeletal protein Lgl. *Nature.* 422:326–330.

Bilder, D., and N. Perrimon. 2000. Localization of apical epithelial determinants by the basolateral PDZ protein Scribble. *Nature.* 403:676–680.

Bilder, D., M. Li, and N. Perrimon. 2000. Cooperative regulation of cell polarity and growth by *Drosophila* tumor suppressors. *Science.* 289:113–116.

Bilder, D., M. Schober, and N. Perrimon. 2003. Integrated activity of PDZ protein complexes regulates epithelial polarity. *Nat. Cell Biol.* 5:53–58.

Cai, Y., F. Yu, S. Lin, W. Chia, and X. Yang. 2003. Apical complex genes control mitotic spindle geometry and relative size of daughter cells in *Drosophila* neuroblast and pI asymmetric divisions. *Cell.* 112:51–62.

Cox, R.T., C. Kirkpatrick, and M. Peifer. 1996. Armadillo is required for adherens junction assembly, cell polarity, and morphogenesis during *Drosophila* embryogenesis. *J. Cell Biol.* 134:133–148.

Doe, C.Q. 2001. Cell polarity: the PARty expands. *Nat. Cell Biol.* 3:E7–E9.

Doe, C.Q., and B. Bowerman. 2001. Asymmetric cell division: fly neuroblast meets worm zygote. *Curr. Opin. Cell Biol.* 13:68–75.

Etemad-Moghadam, B., S. Guo, and K.J. Kemphues. 1995. Asymmetrically distributed PAR-3 protein contributes to cell polarity and spindle alignment in early *C. elegans* embryos. *Cell.* 83:743–752.

Goodman, C.S., and C.Q. Doe. 1993. Embryonic development of the *Drosophila* central nervous system. *In* The Development of *Drosophila melanogaster*. Vol. 2. Cold Spring Harbor Laboratory Press, Cold Spring Harbor, NY. 1131–1206.

Hong, Y., B. Stronach, N. Perrimon, L.Y. Jan, and Y.N. Jan. 2001. *Drosophila* Stardust interacts with Crumbs to control polarity of epithelia but not neuroblasts. *Nature.* 414:634–638.

Humbert, P., S. Russell, and H. Richardson. 2003. Dlg, Scribble and Lgl in cell polarity, cell proliferation and cancer. *Bioessays.* 25:542–553.

Hung, T.J., and K.J. Kemphues. 1999. PAR-6 is a conserved PDZ domain-containing protein that colocalizes with PAR-3 in *Caenorhabditis elegans* embryos. *Development.* 126:127–135.

Jan, Y.N., and L.Y. Jan. 2001. Asymmetric cell division in the *Drosophila* nervous system. *Nat. Rev. Neurosci.* 2:772–779.

Joberty, G., C. Petersen, L. Gao, and I.G. Macara. 2000. The cell-polarity protein Par6 links Par3 and atypical protein kinase C to Cdc42. *Nat. Cell Biol.* 2:531–539.

Kalmes, A., G. Merdes, B. Neumann, D. Strand, and B.M. Mechler. 1996. A serine-kinase associated with the p127-*l(2)gl* tumor suppressor of *Drosophila* may regulate the binding of p127 to nonmuscle myosin II heavy chain and the attachment of p127 to the plasma membrane. *J. Cell Sci.* 109:1359–1368.

Kemphues, K. 2000. PARsing embryonic polarity. *Cell.* 101:345–348.

Knoblich, J.A. 2001. Asymmetric cell division during animal development. *Nat.*

Rev. Mol. Cell Biol. 2:11–20.

Kraut, R., W. Chia, L.Y. Jan, Y.N. Jan, and J.A. Knoblich. 1996. Role of inscuteable in orienting asymmetric cell divisions in *Drosophila*. *Nature.* 383:50–55.

Kuchinke, U., F. Grawe, and E. Knust. 1998. Control of spindle orientation in *Drosophila* by the Par-3-related PDZ-domain protein Bazooka. *Curr. Biol.* 8:1357–1365.

Lee, T., and L. Luo. 2001. Mosaic analysis with a repressible cell marker (MARCM) for *Drosophila* neural development. *Trends Neurosci.* 24:251–254.

Lee, T., C. Winter, S.S. Marticke, A. Lee, and L. Luo. 2000. Essential roles of *Drosophila* RhoA in the regulation of neuroblast proliferation and dendritic but not axonal morphogenesis. *Neuron.* 25:307–316.

Lin, D., A.S. Edwards, J.P. Fawcett, G. Mbamalu, J.D. Scott, and T. Pawson. 2000. A mammalian PAR-3-PAR-6 complex implicated in Cdc42/Rac1 and aPKC signalling and cell polarity. *Nat. Cell Biol.* 2:540–547.

Mathew, D., L.S. Gramates, M. Packard, U. Thomas, D. Bilder, N. Perrimon, M. Gorczyca, and V. Budnik. 2002. Recruitment of Scribble to the synaptic scaffolding complex requires GUK-holder, a novel DLG binding protein. *Curr. Biol.* 12:531–539.

Muller, H.A., and E. Wieschaus. 1996. *armadillo*, *bazooka*, and *stardust* are critical for early stages in formation of the zonula adherens and maintenance of the polarized blastoderm epithelium in *Drosophila*. *J. Cell Biol.* 134:149–163.

Oda, H., T. Uemura, Y. Harada, Y. Iwai, and M. Takeichi. 1994. A *Drosophila* homolog of cadherin associated with armadillo and essential for embryonic cell-cell adhesion. *Dev. Biol.* 165:716–726.

Ohno, S. 2001. Intercellular junctions and cellular polarity: the PAR-aPKC complex, a conserved core cassette playing fundamental roles in cell polarity. *Curr. Opin. Cell Biol.* 13:641–648.

Ohshiro, T., T. Yagami, C. Zhang, and F. Matsuzaki. 2000. Role of cortical tumour-suppressor proteins in asymmetric division of *Drosophila* neuroblast. *Nature.* 408:593–596.

Parnas, D., A.P. Haghighi, R.D. Fetter, S.W. Kim, and C.S. Goodman. 2001. Regulation of postsynaptic structure and protein localization by the Rho-type guanine nucleotide exchange factor dPix. *Neuron.* 32:415–424.

Peng, C.Y., L. Manning, R. Albertson, and C.Q. Doe. 2000. The tumour-suppressor genes *lgl* and *dlg* regulate basal protein targeting in *Drosophila* neuroblasts. *Nature.* 408:596–600.

Petronczki, M., and J.A. Knoblich. 2001. DmPAR-6 directs epithelial polarity and asymmetric cell division of neuroblasts in *Drosophila*. *Nat. Cell Biol.* 3:43–49.

Qiu, R.G., A. Abo, and G. Steven Martin. 2000. A human homolog of the *C. elegans* polarity determinant Par-6 links Rac and Cdc42 to PKCzeta signaling and cell transformation. *Curr. Biol.* 10:697–707.

Schober, M., M. Schaefer, and J.A. Knoblich. 1999. Bazooka recruits Inscuteable to orient asymmetric cell divisions in *Drosophila* neuroblasts. *Nature.* 402: 548–551.

Strand, D., I. Raska, and B.M. Mechler. 1994. The *Drosophila lethal(2)giant larvae* tumor suppressor protein is a component of the cytoskeleton. *J. Cell Biol.* 127:1345–1360.

Suzuki, A., T. Yamanaka, T. Hirose, N. Manabe, K. Mizuno, M. Shimizu, K. Akimoto, Y. Izumi, T. Ohnishi, and S. Ohno. 2001. Atypical protein kinase C is involved in the evolutionarily conserved par protein complex and plays a critical role in establishing epithelia-specific junctional structures. *J. Cell Biol.* 152:1183–1196.

Tabuse, Y., Y. Izumi, F. Piano, K.J. Kemphues, J. Miwa, and S. Ohno. 1998. Atypical protein kinase C cooperates with PAR-3 to establish embryonic polarity in *Caenorhabditis elegans*. *Development.* 125:3607–3614.

Tepass, U., C. Theres, and E. Knust. 1990. crumbs encodes an EGF-like protein expressed on apical membranes of *Drosophila* epithelial cells and required for organization of epithelia. *Cell.* 61:787–799.

Tepass, U., G. Tanentzapf, R. Ward, and R. Fehon. 2001. Epithelial cell polarity and cell junctions in *Drosophila*. *Annu. Rev. Genet.* 35:747–784.

Wodarz, A. 2002. Establishing cell polarity in development. *Nat. Cell Biol.* 4:E39–E44.

Wodarz, A., A. Ramrath, U. Kuchinke, and E. Knust. 1999. Bazooka provides an apical cue for Inscuteable localization in *Drosophila* neuroblasts. *Nature.* 402:544–547.

Wodarz, A., A. Ramrath, A. Grimm, and E. Knust. 2000. *Drosophila* atypical protein kinase C associates with Bazooka and controls polarity of epithelia and neuroblasts. *J. Cell Biol.* 150:1361–1374.

Woods, D.F., and P.J. Bryant. 1991. The discs-large tumor suppressor gene of *Drosophila* encodes a guanylate kinase homolog localized at septate junctions. *Cell.* 66:451–464.

Yamanaka, T., Y. Horikoshi, Y. Sugiyama, C. Ishiyama, A. Suzuki, T. Hirose, A. Iwamatsu, A. Shinohara, and S. Ohno. 2003. Mammalian Lgl forms a protein complex with PAR-6 and aPKC independently of PAR-3 to regulate epithelial cell polarity. *Curr. Biol.* 13:734–743.

Yu, F., X. Morin, Y. Cai, X. Yang, and W. Chia. 2000. Analysis of partner of inscuteable, a novel player of *Drosophila* asymmetric divisions, reveals two distinct steps in inscuteable apical localization. *Cell.* 100:399–409.